5-2024

Retrieving images from tarnished daguerreotypes using X-ray fluorescence imaging with an X-ray micro beam with tunable energy

Tsun-Kong Sham

Y. Zou Finfrock

Qunfeng Xiao

Renfei Feng

Sarah Bassnett
Western University, sarah.bassnett@uwo.ca

Journal of Cultural Heritage 67 (2024) 53–61

Contents lists available at ScienceDirect

Journal of Cultural Heritage

journal homepage: www.elsevier.com/locate/culher

Original article

Retrieving images from tarnished daguerreotypes using X-ray fluorescence imaging with an X-ray micro beam with tunable energy

Tsun-Kong Sham[a,*], Y. Zou Finfrock[b], Qunfeng Xiao[c], Renfei Feng[c], Sarah Bassnett[d]

[a] Department of Chemistry, Western University, London, ON, N6A 5B7 Canada
[b] X-ray Science Division, Advanced Photon Source, Argonne National Laboratory, Argonne, IL 60439, USA
[c] Canadian Light Source, Saskatoon, SK, S7N 2V3, Canada
[d] Department of Visual Arts, Western University, London, ON, N6A 5B7 Canada

ARTICLE INFO

Article history:
Received 13 September 2023
Revised 6 January 2024
Accepted 6 February 2024

Keywords:
Daguerreotypes
Tarnish
Conservation
Hard X-ray
Tender X-ray
Imaging
Microspectroscopy

ABSTRACT

We report recent observations using a synchrotron X-ray micro-beam to retrieve images from tarnished 19th century daguerreotypes. We confirm that high quality image can always be retrieved from tarnished plates using Hg L_α XRF as long as the bulk of the image particles and their distribution remains intact. We also report results from using tunable tender X-rays (2 - 7 keV) to conduct imaging in high vacuum at energy above the Ag L-edge and the Hg M-edge, extracting images using Ag L_α and Hg M_α, respectively among others (e.g., S to track corrosion). Images obtained with the surface sensitive total electron yield (TEY) and the bulk sensitive fluorescence yield (FLY) as well as corresponding micro-XANES are reported. Flux tolerance to high intensity X-beam is also explored. These results and their implications for cultural heritage research are discussed.

1. Introduction: the daguerreotype

1.1. History and significance of daguerreotypes

The daguerreotype process was the first commercially viable form of photography, and it was invented in France by Joseph Nicéphore Niépce (1765–1833) and Louis-Jacques-Mandé Daguerre (1787–1851). Daguerreotypes are one-of-a-kind, positive images made on thin sheets of silver-plated copper. Because of their fragile surface, they were usually covered with glass and kept in frames or cases, giving them a precious quality. Introduced in 1839, this new method of image making quickly captured public interest and was sought-after until the mid-1850s, when it was gradually replaced with paper photographs [1–5]. Daguerreotypy became a global industry that transformed image making and changed the way people thought about themselves, the world, and their relationship to others [3].

Portraiture was the most popular subject matter for daguerreotypes. At first, long exposure times made it difficult to achieve good results, but improvements in chemistry and equipment soon changed that [5]. More affordable than painted portraits and resulting in more detailed and realistic likenesses than other non-photographic process such as silhouettes, daguerreotypes were a new and modern way of representing the self. The market for portraiture was stimulated by a growing awareness among the urban middle class of the way appearance signalled social standing; however, enthusiasm for daguerreotypes was not specific to any one class or cultural group. The best photographic portraits honour, elevate, and celebrate a sitter's positive attributes [3]. Daguerreotypes hold significant artistic, cultural, and historical value, and efforts to preserve and restore these images have aroused considerable interest in the art preservation community [6–9].

Production of a daguerreotype image requires several steps. The result is a sharp contrast, a one-of-a-kind photograph. The process begins with making a finely polished silver-coated copper plate; this is followed by the exposure of the surface to iodine, making the plate photosensitive upon the formation of silver iodide. Later variations utilized alternative halogens, such as chlorine, bromine, or a combination, to increase the sensitivity of the surface to light. The photosensitive plate is mounted in the lightproof interior of a camera; then the lens cap is removed, exposing the plate to light (often requiring several minutes!). This step causes the formation of silver image particles that result from photolysis of the silver halide on the silver surface, creating the image. Areas with dense

* Corresponding author.
E-mail address: tsham@uwo.ca (T.-K. Sham).

https://doi.org/10.1016/j.culher.2024.02.003

distributions of image particles of uniform shape and size correspond to high light intensity, whereas areas exposed to low light intensity display thin and nonuniform image particles. Bright regions are the result of the particles scattering light, and where there are few image particles, only light from specular reflection can be seen. Therefore, the light and dark areas can change if the daguerreotype is tilted. After the image has formed on the surface, the plate is then exposed to mercury vapor, which fixes the image on the silver-coated copper plate. This is the crucial step in the entire process and, as we shall show below, the presence of Hg on the image particles allows us to retrieve the delicate details of the image from a tarnished daguerreotype. Excess halides are removed with a salt solution, such as sodium thiosulfate. This makes the surface insensitive to light and halts the creation of additional image particles. Next, the silver-coated copper plate is washed with distilled water, and a gold chloride solution is poured on the daguerreotype to ensure the longevity and durability of the image. The addition of the gold chloride, this step, known as gilding, was later introduced into the final stages of the daguerreotype process. Finally, the plate is heated to dry the surface. This process produces a completed daguerreotype image of the object.

1.2. Deterioration of the daguerreotype

Daguerreotypes are subject to formation of a surface tarnish due to corrosion which, in the extreme, can completely obscure the image. Surface corrosion alters the shape and refractivity of the image particles, hence the direction and intensity of the scattered light. The most frequent tarnishes (corrosion products) are silver halides, silver oxides and sulfur compounds originating from incomplete washing during the original preparation, exposure to ambient gases and deterioration of the cover glass [6–9]. Studies have also focused on the effects of the daguerreotype storage and exposure conditions. Extreme temperatures and humidity can have a negative influence on the integrity of the surface. When a daguerreotype is stored, a glass cover is usually present on the image side of the surface; however, deterioration of the glass cover can be another factor contributing to degradation of the plate. Many original glasses cover plates contained sodium and potassium, which have been shown over time to diffuse from the glass and leave deposits on the daguerreotype surface. This leads to highly localized spots of corrosion across the daguerreotype. In addition, the glue that was used to adhere the glass cover to the plate also contributed to corrosion at the perimeter of the daguerreotypes [1–5].

1.3. Conservation and preservation methods

Daguerreotypes were fragile, and Daguerre himself recommended that the plate be protected with a cover glass. About twenty years after their invention, the commercial production of daguerreotypes was no longer practiced; and they became collectors' items. It was not until the twentieth century that archives, and art institutions began collecting and preserving daguerreotypes [1–5]. Many preservation and restoration processes have been tried with varying success. Due to variations in the methods of preparation as well as diverse storage conditions, many daguerreotypes have unique damage requiring tailored cleaning methods. As a result, there is not a single method guaranteed to restore these images. While progress has been made, these procedures completely depend on the original quality of the plate and its surface. There are two general cleaning techniques: chemical cleaning and electro cleaning. There are also two common methods in electro cleaning, sometimes referred to as the Wei and the Barger method [10–12]. The Wei method simply applies a cathodic polarization to the daguerreotype plate in a cleaning solution [10]. The Barger method applies both oxidizing and reducing polarizations to induce anodic and cathodic currents on the daguerreotype, switching between the two throughout the process [11,12]. It is hoped that by manipulating the surface chemistry, the tarnish will be removed, while the image particles (nano particles of Ag coated with Hg forming an amalgam) will remain intact. Numerous studies have proven that both methods can help restore the daguerreotype image only to some extent. However, since each daguerreotype is unique in terms of the composition of the tarnish and how deteriorated it is, the methods are not always effective, because the surface corrosion is inhomogeneous. In some cases, electro-cleaning treatments have resulted in further damage to the daguerreotype.

1.4. Breakthrough in Hg L_α XRF imaging using a micro focused synchrotron X-ray beam

Synchrotron X-ray, because of its tunability, brightness and collimation, allows us to excite a specific element of interest preferentially, by tuning the excitation energy to just above the threshold of a core electron of interest, known as an absorption edge where the absorption of the X-ray of the element of interest increases abruptly; for example, the K-edge of S (exciting a 1 s electron to the continuum) or the L_3-edge of Hg (exciting a $2p_{3/2}$ electron to the continuum). The core hole left behind is subsequently filled by electrons in the upper levels, emitting the energy as an X-ray characteristic of the element. This process is known as X-ray fluorescence (XRF). Thus, by scanning a focused micron size X-ray beam with the desired energy across the specimen, pixel by pixel, and monitoring the yield of the characteristic XRF, we can map the element distribution of the specimen. In 2018, using a micro-focused X-ray beam, selecting the excitation energy to just above the Hg L_3-edge and tracking the Hg L_α and L_β XRF lines in a two-dimensional scan across a daguerreotype plate, we succeeded in retrieving the original image in its entirety from daguerreotypes tarnished beyond recognition [13].

These results and subsequent work [14–18] show that the Hg L_α XRF method works if the integrity of the bulk of silver image particles remains physically intact. These image particles formed upon light induced photochemical reaction of the photosensitizer (silver halide), and the subsequent exposure to hot Hg vapor [13–18] Hg vapor stabilizes the image particles of silver clusters forming an amalgam, of which, the shape and density define the image, and the image particles are preserved by the presence of Hg. Since surface corrosion causes tarnish, which is inhomogeneous, cleaning methods will never achieve the desired effect of retrieving the original image in its entirety [18]. However, surface reactions of adventitious contaminants, such as sulfur or organic molecules from the ambient environment, only alter the chemical composition of the surface and the near-surface region ($\sim$ nm). This would change the reflectivity of visible light but have little adverse effect on the bulk of the image particles. Therefore, the image can be recovered from monitoring the Hg L_α fluorescence X-rays. This can only be conducted effectively using synchrotron radiation to provide a microbeam at selected X-ray energy (often just above the Hg L_3 edge, e.g., 13 keV to enhance the absorption by Hg). The ability to retrieve clear images from a tarnish plate with this XRF technique was further demonstrated in several subsequent studies where we successfully retrieved fine images from 19th century daguerreotypes tarnished beyond recognition and accessing how chemical and electrical cleaning may affect the quality of the image in preservation and conservation [15–18].

We also made another amazing observation when we scanned the daguerreotype plate using a micro beam of tender X-rays ($\sim$ 3.5 keV) at energy just above the Ag L_3-edge (E_o = 3351 eV) [14,15]. We were able to retrieve a clear image of the obscured

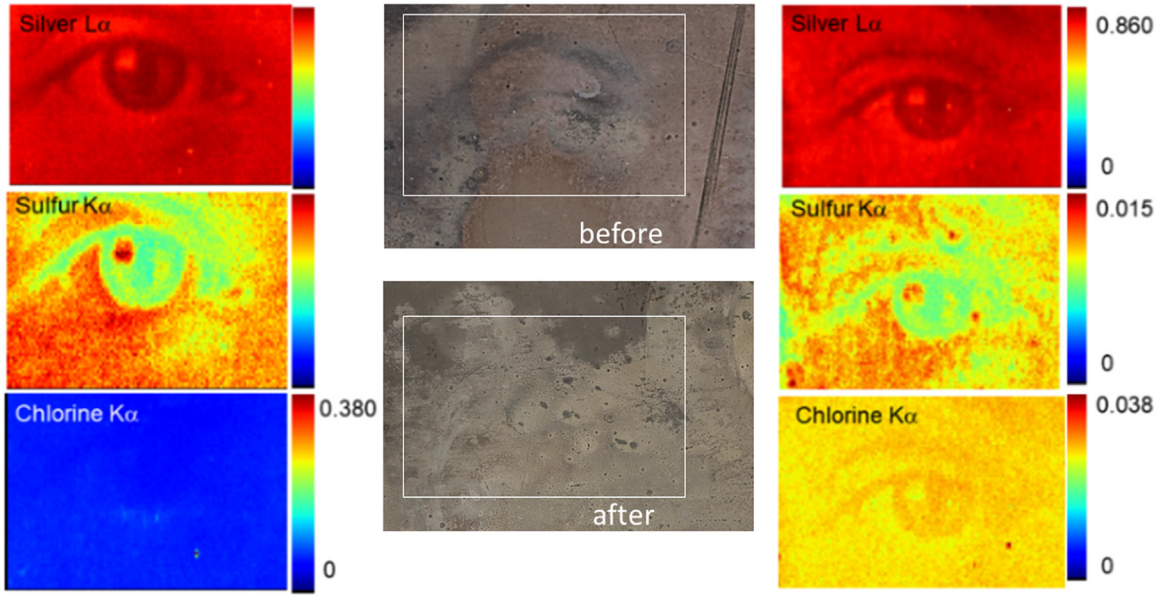

Fig. 1. Left and right panel (from top to bottom): Ag L_α, S K_α and Cl K_α XRF images from a tarnished plate before and after electrocleaning (mid panel) with a 10 μm × 10 μm X-ray beam at 3.5 keV; the rectangle marks the area of interest. Results taken from Madalena Kozachuk et al., references 14 and 15.

eye in the portrait of a lady even though the substrate is Ag. Fig. 1 shows the image of the eye of the plate before and after electrocleaning. It is interesting to note that this is a situation where cleaning further obscured the face completely (mid-section), yet Ag L_α XRF still produces a nice image (right section). This works because the penetration depth of the X-ray at these tender X-ray energies is shallow, the incident X-ray is largely absorbed by the surface image particles. Thus, it tracks predominately the surface Ag image particles, hence the image. It is also found that the S signal is most intense in the high-density areas of image particles, while Cl has a more homogeneous distribution [14,15].

1.5. Objectives and organization of the manuscript

In this paper, we present recent studies to further confirm the importance of the integrity of the bulk of the image particles of daguerreotype, which allows for the retrieval of clear images from Hg L_α and Ag L_α XRF at hard and tender X-ray energies, respectively, despite surface corrosion. In Section 2, we describe the history of the daguerreotype plates and synchrotron radiation methodology. We explore the limitations of the techniques in Section 3 with respect to (1) flux tolerance and radiation damages, (2) tender vs soft X-ray imaging, (3) imaging under vacuum using the surface sensitive Total Electron Yield (TEY) mode vs. the bulk sensitive Fluorescence Yield (FLY) mode and (4) implication for the materiality in art and cultural significance of these studies. Conclusions and prospects are presented in Section 4.

2. Materials and methodology

2.1. Daguerreotype plates

The 19th century daguerreotype plates were either provided by the National Gallery of Canada (NGC) in Ottawa or purchased from private collectors recommended by experts (John McElhone the former Photographs Conservator at the NGC). These plates are all partially tarnished. Optical images of these plates will be displayed below with the source noted in the figure caption. The plates obtained from private collectors were in a case and protected with a cover glass. These plates were removed from the case. Herein we focus on the technical aspects for retrieving the image from a tarnished daguerreotype and establishing the technique's advantages and limitations. All the plates were evaluated as is without any surface treatment.

2.2. Synchrotron beamlines and end-station instrumentation for XRF imaging

Synchrotron XRF imaging techniques have been developed for cultural heritage study for some time, especially in tracking paintings [19–21], ancient artifacts [21–24] and manuscripts [25] among many applications [26,27]. The application of synchrotron XRF imaging to retrieve images from tarnished daguerreotypes is more recent [14–16]. Herein we will focus on the technical aspects and expand the imaging work to the soft and tender X-ray region.

Three synchrotron beamlines have been used for these studies. The Sector 20 ID (insertion device) beamline of the X-ray Science Division (XSD) at the Advanced Photon Source (APS) of the Argonne National Laboratory, which also hosts the Canadian Light Source (CLS) offshore facility, CLS@APS. This beamline is equipped with KB mirrors and can focus the beam to 5 μm [28]. The other two beamlines are the Soft X-ray Materials Analysis Beamline (SXRMB) and the Very Sensitive Elemental and Structural Probe Employing Radiation from a Synchrotron (VESPERS) beamline at the CLS [29,30]. SXRMB is unique in that it provides tender X-rays (~2- 5 keV) for imaging, and the specimen is housed in a vacuum chamber with the added advantage that surface sensitive electron yield signals can be used to track the images; more on this will be discussed below. A beam of ~ 10 μm × 10 μm and 5 μm × 5 μm can be routinely produced at the SXRMB and VESPERS, respectively. Typical scan at the 20 ID line and SXRMB uses a 25–50 μm beam and at the VESPER a 5 μm × 5 μm beam with varying step size from 25 to 100 μm to optimize the acquisition time.

In hard X-ray imaging, we used an excitation energy of 13.5 keV, which is just above the Hg L_3-edge (12,284 eV) as well as the Br K-edge (13,474 eV) and tracked the Hg L_α X-ray fluorescence (9989 eV) as well as the Au L_α and Br K_α. In tender X-ray imaging, we varied the photon energy from 2.5 keV to 7 keV which allows us to vary the photon penetration depth with access to Ag image particles at excitation above the Ag L_3-edge (3351 eV)

and K-edges of elements responsible for surface corrosion such as S (2472 eV) and Cl (2822 eV) by tracking the S K_α (2307 eV) and Cl K_α (2622 eV), respectively (Fig. 1).

The fluorescence signal was recorded with a silicon drift detector (SDD) at 20 ID, SXRMB and VESPERS, a Pilatus 400 area sensitive detector was also available at the VESPERS. The X-ray fluorescence spectrum was stored in a multichannel analyzer (MCA) and energy windows at appropriate fluorescence energies were selected to create the elemental maps of interest pixel by pixel.

3. Results and discussion

3.1. Is daguerreotype high flux tolerant and is radiation damage an issue?

Let us begin by asking the question of whether radiation damage is an issue in these analyses with high photon intensity. At first glance, this does not appear to be an issue because, unlike non-conducting solids and soft molecular materials, a daguerreotype plate is made of metal (Ag coated Cu) and the sample is grounded, so there are no charging issues, and radiation chemistry is limited to the surface. We have not observed any noticeable radiation damage in our previous studies until this report [13–18]. We will elaborate on this below. Of the three beamlines, the 20 ID line is based on an undulator, while SXRMB and VESPERS are both on bending magnets. The ID line will be orders of magnitude, typically $\sim 10^{12}$ photons/sec with 50 × 50 μm^2 spot size, more intense than the bending magnet source at VESPER and SXRMB for comparable beam size and ring current ($\sim 10^9$ photons/s).

It is apparent from Fig. 2 that once again, what was obscured under the tarnished area has been revealed in the Hg L_α XRF map. In fact, the entire image of an elegant lady, including her expression, hair style and dress emerges with delicate details. The portrait tracked with Ag L_α is barely noticeable because it is masked by the Ag substrate signal which only contribute to the background (hard X-ray penetrates the image particle layer into the bulk). Ag L-edges and corresponding L_α XRF are in the tender X-ray region, further discussion on this will be provided in Section 3.2, Au L_α also reveals the image albeit somewhat obscured. This is expected since the hot Hg vapor targets the image particles during fixing and the forming of the amalgam Hg-Ag image particles, while Au was applied later after the image was fixed and Au interacted indiscriminately with the plate in the gliding process. The Br K_α map (not shown) from the residual photosensitizer shows similar pattern as that of Au. Once again, we have successfully retrieved the fine image from a tarnished daguerreotype. This is possible because the image particles remain intact in the bulk despite surface corrosion, hence their distribution also remains intact, yielding a clear Hg L_α image since the XRF detected by the SDD detector is only element, not chemical sensitive. A closer scrutiny at the Hg XRF image, however, reveals a black spot on the left eyebrow of the lady, which is not seen in the optical image prior to the scan. In another X-ray confocal line scan experiment, we also observed a black spot. Thus, for the very first time, we observed visible damage on the daguerreotype induced by X-rays! In the confocal scan, we track the XRF from a region of the specimen using a focused beam of ~ 2 - 3 μm (10^{11} photons/s) and a special optic to obtain a two-dimensional scan. The optic blocks X-rays from undesired regions to reach the detector [31,32].

Fig. 3 shows the visibly damaged daguerreotypes images after exposure to an intense X-ray beam during a normal and confocal line scan and the corresponding XRF maps.

Comparing the optical images of Figs. 2 and 3, visible damage in the ROI is optically unmistakable, especially around the left eye. The damage appears to proliferate beyond both sides of the line. As noted above, upon closer examination of the Hg map (Figs. 2(a) and 3 (a)) before the line scan, a black spot is also visible on the left eyebrow. A black spot represents loss of material (low absorption) as if the material is evaporated. To find out whether the image particles are destroyed in the vicinity of the line after confocal scan, we ran a normal XRF scan again on the optically damaged plate, and the results are shown in Figure (c)-(f).

It is interesting to note that the proliferated damage clearly visible in the optical image after the line scan is not reproduced in the Hg nor Au XRF image. Figs. 3(c) and (d) show a well-resolved image, except for another black spot at the beginning of the line scan and a very thin line along the direction of the scan. This observation is reassuring because, except for a few spots, high flux, altering the surface chemistry noticeably, has negligible effect on the bulk of the image particles over most of the ROI and clear images can still be retrieved even if it appears damaged optically. We now envisage what may cause the black spot. As noted above, the 20 ID line is the most intense source (at least one order of magnitude) among all the sources we had previously used at CHESS and at CLS (all bending magnet). We speculate that X-ray absorption is unusually strong at these spots, possibly due to impurities or corrosion products, and subsequent chemistry generates heat locally. This heat can induce further alloying and mass diffusion away from the spot on the surface of the plate, resulting in the proliferation of the damage optically (changing the surface reflectivity markedly). Additional evidence awaits further investigation.

Fig. 2. A 19th century daguerreotype of the portrait of a lady from the collection of NGC in Ottawa. From left to right, the photo of the plate, the Hg L_α XRF map, the Ag L_α and the Au L_α XRF map recorded at the 20 ID beamline of the APS using a 50 μm × 50 μm beam at 13.5 keV, with 50 μm steps and 200 ms integration time.

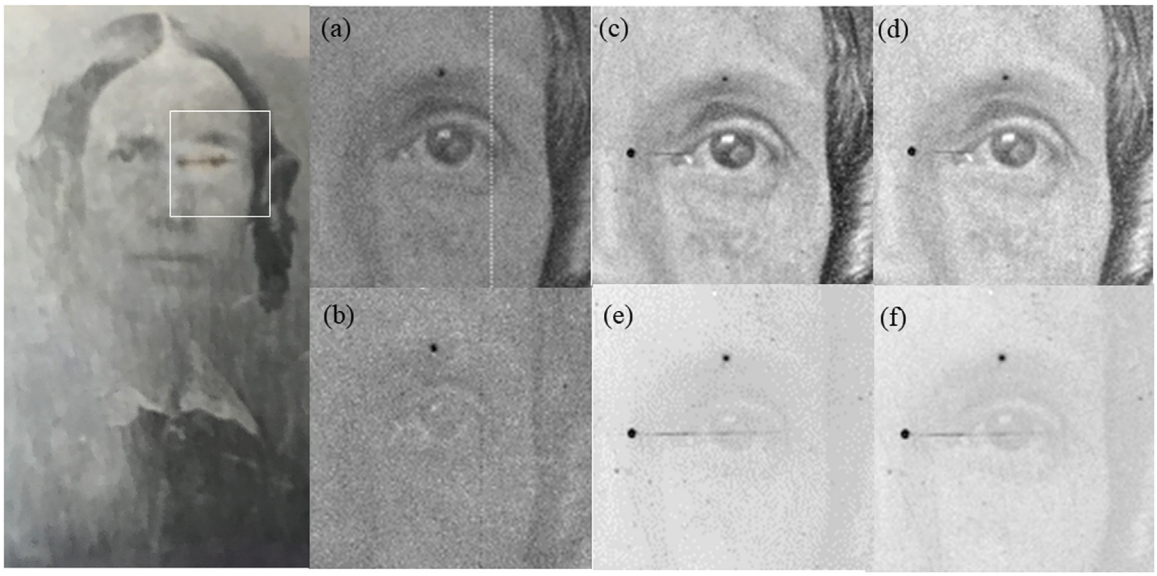

Fig. 3. Left: optical image of the daguerreotype (Fig. 2) after a confocal line scan; the visibly damaged region of interest (ROI) is marked with a square. Right: (a) and (b): the Hg and Au L_α XRF map, respectively, of the ROI before the line scan. (c) and (d): the Hg L_α and L_β XRF map after the line scan; (e) and (f): the Au L_α and L_β XRF map after the line scan. The use of L_β reduces the overlap of Hg and Au XRF.

3.2. Tender versus hard X-rays

We ventured into systematic tender X-ray (2 - 5 keV) imaging, which can only be performed efficiently in helium or in vacuum. At SXRMB, imaging is conducted in high vacuum ($\sim 10^{-6}$ – 10^{-7} torr); [29] this provides the added advantage of being able to obtain the image with total electron yield as well. This will be discussed in the next section.

We first consider the penetration depth of tender vs hard X-rays. Fig. 4(a) displays the X-ray attenuation length of X-ray energies at the Hg L_3 -edge (hard X-ray), the Ag L_3 and Hg M -edges (tender X-ray) as well as the attenuation length of their corresponding XRF for a HgAg alloy ($Ag_{11}Hg_9$, a stable phase at room temperature). The experimental setup is also shown in Fig. 4(b) where the scan stage can be viewed from the top. Fig. 4(c) shows how a plate is mounted. The specimen is grounded so that the total electron yield can be measured as the drained current.

Fig. 4(a) shows that hard X-rays penetrate (e.g., ~ 10 μm at the Hg L_3-edge, at ~ 13 keV) into the specimen well beyond the thin layer of the image particles (~ order of 10 to 10^2 nm). Tender X-rays (e.g., ~ 500 nm at the Ag L_3 and Hg M_3 -edges of ~ 3.4 keV and 2.7 keV, respectively) are largely absorbed by the surface layer of the image particles, thus, one expects that the Ag L_α and Hg M_α XRF can both yield a clean image if the bulk of the image particles remains intact. On the other hand, X-ray above the Hg L_3-edge (13.5 keV) where Hg absorption is maximized, will uncover the image with a huge background (Fig. 2).

Figs. 5 and 6 show two 19th century daguerreotype plates from private collection, and they have been imaged with both tender and hard X-rays @ the SXRMB and VESPERS beamline of the CLS, respectively.

The optical image in Fig. 5 shows a tarnished portrait of a lady with three easily identifiable spots in the forehead between the eyes, along with other scattered dark spots. From Figs. 5(a) (Ag L_α) and (b) (S K_α), one can clearly see that the Ag L_α XRF map retrieves a clear image without the three dark spots between the eyes. This indicates that these spots are surface impurities with Ag content which are indistinguishable from pure Ag in XRF mapping with a SDD detector of moderate energy resolution; the S K_α XRF map shows these dark spots and confirms they are of sulfur origin. It is interesting to note that the Ag L_α map excited at 3.5 keV produces considerably better contrast than that excited at 13.5 keV (Fig. 2) because the contribution from the Ag substrate is significantly reduced in the former. Figs. 5(c) and 5 (d) show the Hg L_α

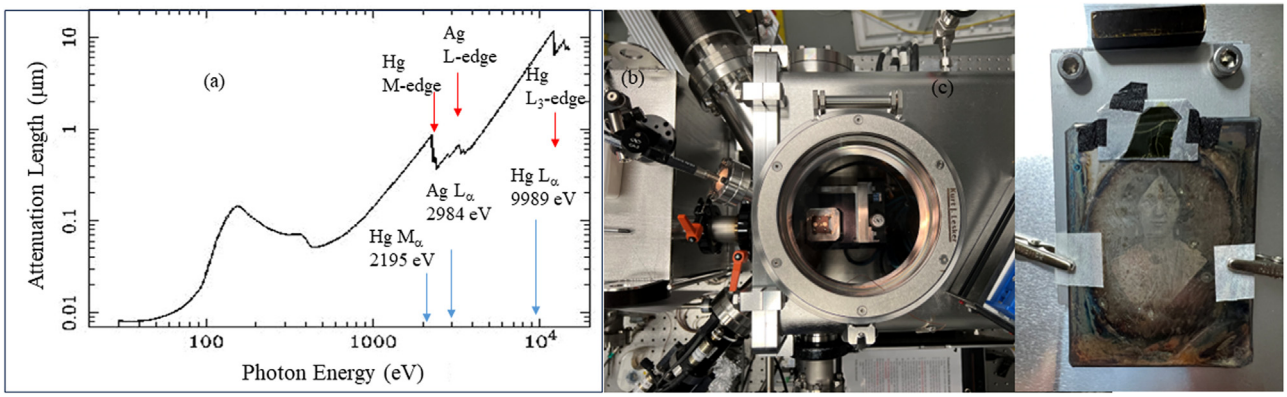

Fig. 4. (a) Attenuation length at relevant X-rays energies as marked (red arrow: edge; blue arrow, XRF). Data: https://henke.lbl.gov/optical_constants/ (b) Top view of the microprobe. (c) The specimen is mounted on a flat stainless plate fastened on the scanning stage; the sample is connected to a current amplifier so that electron current yield can be measured.

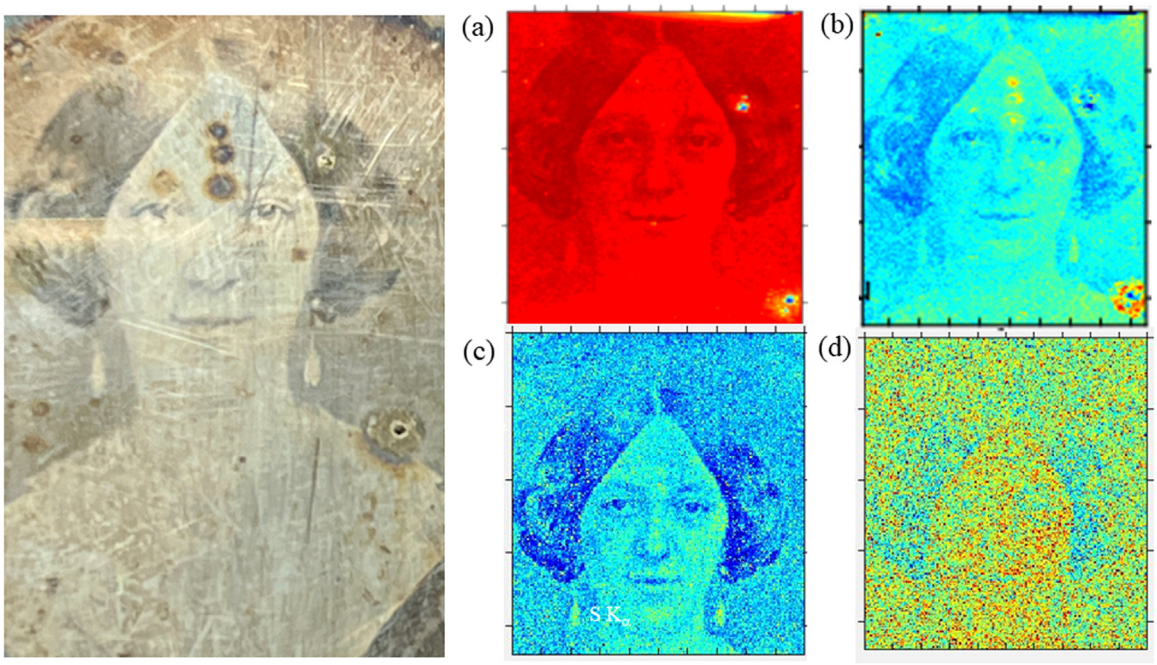

Fig. 5. Left: Optical image of the portrait of an elegant lady from private collection. Right: (a) and (b) are Ag L_α (1978 eV) and S K_α (2398 eV) XRF map (20 mm × 25 mm), respectively obtained at SXRMB with a 10 μm × 10 μm beam at the energy of 3.5 keV, (Ag L_3-edge: 3343 eV; S K-edge: 2472 eV); (c) and (d) are Hg L_α (9989 e V) and Br K_α (11,924 eV) XRF map, respectively, obtained at VESPERS with a 5 μm × 5 μm beam at the energy of 13.5 keV (Hg L_3-edge is at 12,284 eV).

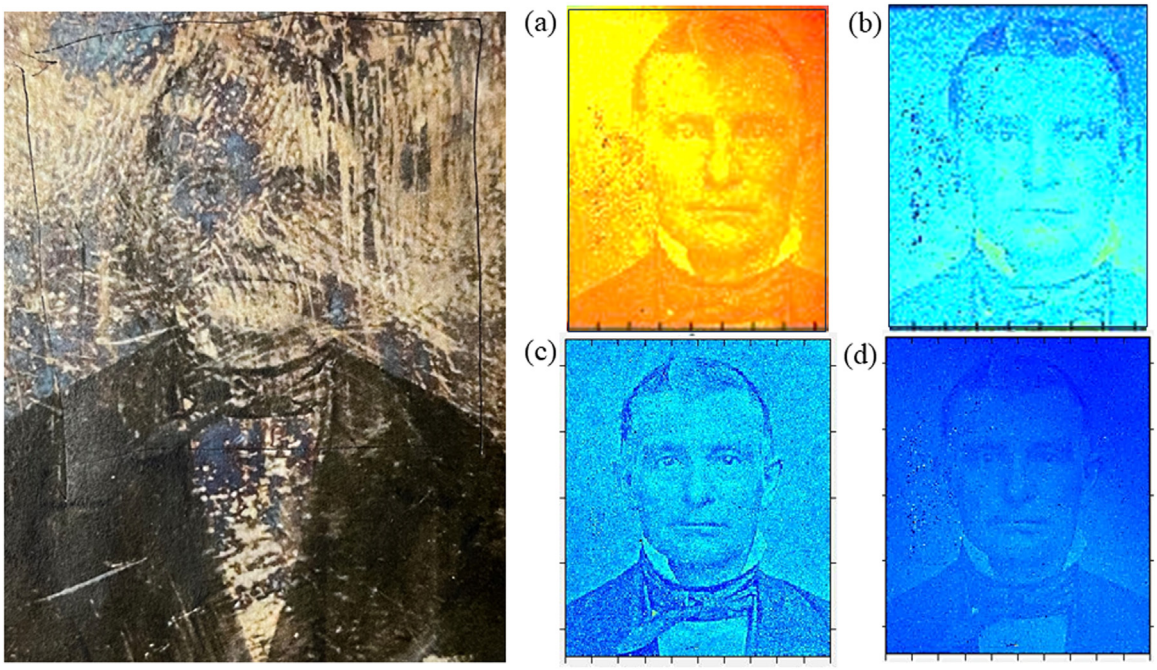

Fig. 6. Left: Optical image of a portrait of a gentleman from private collection. Right: (a) and (b) are Ag $L_{\alpha 1}$ (2978 eV) and Hg $M_{\alpha 1}$ (2398 eV) XRF map (20 mm × 25 mm), respectively obtained at SXRMB with a 10 μm × 10 μm beam at the energy of 3370 eV, (Ag L_3-edge: 3343 eV; Hg M_3-edge: 2847 eV); (c) and (d) are Hg $L_{\alpha 1}$ (9989 eV) and Au $L_{\alpha 1}$ (9713 eV) XRF map obtained at VESPERS with a 5 μm × 5 μm beam at the energy of 13.5 keV (Hg L_3-edge is at 12,284 eV).

map excited at 13.5 keV together with that from Br K_α. Once again, the Hg L_α map produces the best image as reported previously, no dark spots between the eyes for the same reason as noted above in the case of Ag map, and there is little Br left in this case.

Fig. 6 is the portrait of a gentleman with his face mostly tarnished. Figs. 6(a) and (b) display the Ag L_α and Hg M_α. images, respectively excited at energy (3370 eV) just above the Ag L_3 edge. Both clearly reveal the face showing his hair style, and expression, as well as his suits. Both images show that the region around the right ear is burry, indicating that corrosion is more serious in this region and that either the image particles are destroyed or the contribution from corrosion products containing Ag and Hg have detached and masked the surface of this region. Figs. 6(c) and (d) show the Hg and Au L_α XRF image, respectively excited at 13.5 keV. Once again, the Hg L_α map shows the best image as anticipated and the obscured region near the right ear is fully revealed. This observation provides evidence that the images particles around the right ear are largely intact in the bulk and surface

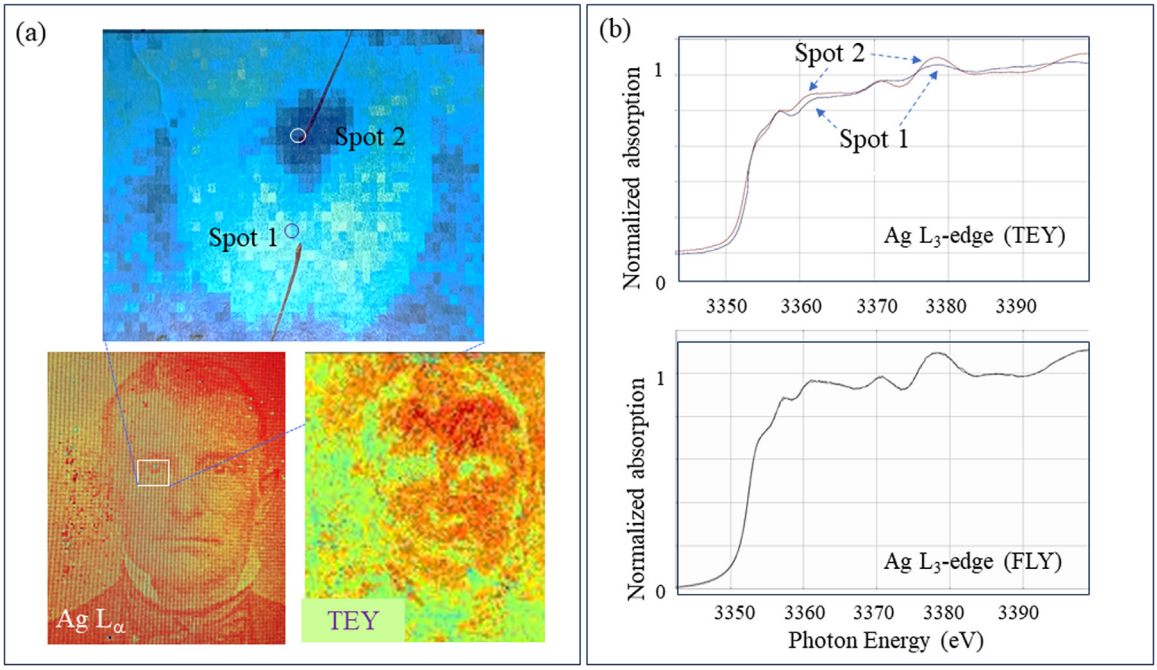

Fig. 7. (a) XRF images of the gentleman shown in Fig. 6 recorded in Ag L_α and TEY together with a fine scan in the region of the right eye (1.2 mm × 1.0 mm) with 3370 eV excitation. Micro XANES at the Ag L_3 -edge were obtained with TEY and FLY at a light and dark spot of the eyeball labelled spot 1 and spot 2, respectively. (b) Ag L_3-edge XANES with a 50 μm × 50 μm, at spot 1 and spot 2 using both TEY and FLY.

Fig. 8. From left to right, the ladies feature in Figs. 2 and 5 and the gentleman in Fig. 6, as well as the optical (tarnished) and the Hg L_α retrieved daguerreotype image of a baby (courtesy of NGC) at 13 keV photon energy at the ID20 line of the APS.

contaminants are largely unmasked in the Hg L_α image using hard X-rays.

3.3. Detecting images using total electron yield (TEY) vs fluorescence yield (FLY)

As noted above, the first use of tunable tender X-rays for imaging in high vacuum allows for further scrutiny of daguerreotype plate from different perspectives. For example, one can tune the photon energy to below and above an edge of interest (Hg M-edge, Ag L-edge, and S K-edge, etc.) and image with different XRF lines. One can also track the image with both total electron yield (TEY) vs fluorescence yield (FLY), which in turn can be used to conduct X-ray Absorption Near Edge Spectroscopy (XANES) with micron spatial resolution.

Fig. 7 illustrates several aspects of tender X-ray imaging and micro-spectroscopy using surface and bulk sensitive measurements. In Fig. 7(a) we can observe that the TEY shows the general

outline of the image which is negative and nonuniform. As TEY tracks total electron yield, which includes a significant contribution from secondary electrons; the region with a high density of image particles (light) produces low TEY, while the dark region with a low density of image particles produces high TEY. The local chemical environment will also affect the TEY, as can be observed from the micro XANES shown in Fig. 7(b) where the Ag L_3-edge XANES recorded in TEY are noticeably different, i.e., that while both are silver metal like, spot 1 exhibits broadening, indicating an inhomogeneous surface; the FYL XANES yield identical spectra at both spots indicating that the composition of the bulk at both spots are identical.

3.4. The cultural heritage significance of recovering tarnished daguerreotypes

While the focus of the article is on the technical aspects of retrieving images from tarnished daguerreotypes, in this section we briefly consider the significance of that retrieval process for cultural heritage. As noted above, daguerreotypes were the predominant form of commercial photography from 1839 until the introduction of paper-based photographic processes in the1850s. There are extensive collections of daguerreotypes in public museums, galleries, and archives around the world, including at the National Gallery of Canada and the Metropolitan Museum of Art. In addition, there are many daguerreotypes in private collections. Some are in excellent condition, but others are not. Retrieving the images from those that are tarnished would greatly increase their value as cultural heritage.

The purpose of museums and other cultural institutions is to collect, preserve, interpret, and display objects of cultural significance. When daguerreotypes develop surface tarnish due to corrosion, they lose much of their value because they cannot be effectively studied or displayed. Retrieving images from daguerreotypes therefore recovers their value as cultural heritage. In some cases, sitters are public figures such as politicians, entertainers, artists, or authors, and these portraits offer insight into their lives. In other cases, such as in the examples retrieved from tarnished plates discussed in this article, sitters are unidentified. Fig. 8 collects the portraits discussed above for easy comparison. The tarnished optical and the Hg L_α images of a baby are also shown. These examples are representative of the type of images produced with the daguerreotype process, and they tell us who was photographed and how they presented themselves. They offer insight into the conventions of appearance as they relate to race, class, gender, and other identity categories and allow historians of photography and other researchers to consider the variety of techniques photographers used, such as lighting, pose, props, and background, to achieve a flattering portrait that conveys aspects of a sitter's character [27]. The advancements in retrieving images from tarnished daguerreotypes discussed in this article are important for conservation efforts and could contribute to the development of protocols for daguerreotype preservation.

4. Conclusion and outlook

We have reported some recent observations in retrieving images from tarnished daguerreotypes using synchrotron X-rays since the 2018 report [13]. We confirm that images can always be retrieved from tarnished daguerreotypes as long as the bulk of the image particles remains intact. Under this condition, surface Hg/Ag containing corrosion and impurities remained attached. They would contribute to the Hg L_α XRF image, as they are part of the elemental signal. Thus, while optical image is strongly affected by surface corrosion (change of refractivity), XRF detection is not affected. We have also addressed the flux tolerance issues which are often ignored since the daguerreotype is a well-polished metal plate. We report the observation of radiation damage for the first time with a strong beam from an ID line. Fortunately, it only appears at a couple of trouble spots of nonconducting surface corrosion products or contaminants from the ambience. We proposed that intense heat generated following strong X-ray absorption facilitates the materials at these spots to diffuse on the surface. More work is required to evaluate this notion. Currently, it is safe to conduct the Hg L_α XRF imaging at 13.5 keV with a modest beam size, e.g., at $\sim$ 25 μm, and modest flux (10^{8} –10^{9} photons/s) at all beamlines.

We have also explored tender X-ray imaging in high vacuum and the effect of photon energy between 2.5 to 7 keV which covers many important edges such as Ag L, Hg M for daguerreotype and S and Cl and K K-edge for the contaminant (e.g., Ag_2S, AgCl and KCl). It is found that we can also retrieve image from tarnished daguerreotype from Ag L_α and Hg M_α with excitation energy above the corresponding L and M edges, e.g., at 3370 eV with a micro beam. However, the same cannot be said for Ag L_α image with hard X-ray (e.g., ~13 keV), as it is masked by a substantial background contribution. We can track the image with total electron yield as well when operated in the vacuum chamber, which in turn allows for surface sensitive (TEY) and bulk sensitive (FLY) micro spectroscopy. Finally, we also note that the images retrieved from these techniques provide valuable information for historians and artists to investigate the life and time of people of that era.

Moving forward, we will continue to explore tarnished 19th century daguerreotypes holistically in tracking every materials aspect of making and preserving daguerreotypes as well as the cause of deterioration using these synchrotron techniques. The physical existence of the plate and the retrieved image will be subjected to its historical interpretation and aesthetic experience. It must be noted that collaboration in this undertaking is essential and will enable the transfer of knowledge and technique to colleagues in the community to help establish protocols for the use of these powerful tools. We are certain that this technique will lead to new insight into the objects under investigation both in their precise physical existence and materiality. More importantly, we envisage that with increasing accessibility to advanced light sources worldwide, this and relating techniques will provide new opportunity for research and training of students, young researchers and technical staff from museums, galleries, and conservation laboratories to become proficient in using synchrotron radiation, and in turn, the emergence of a new breed of researchers and a thriving community [28–34].

Acknowledgments

This research used resources of the Advanced Photon Source (APS); an Office of Science User Facility operated for the U.S. Department of Energy (DOE) Office of Science by Argonne National Laboratory and was supported by the U.S. DOE under contract no DEAC02-06CH11357. XRF imaging was also conducted at the SXRMB and VESPRS microprobes of the Canadian Light Source, which is supported by the Canada Foundation for Innovation (CFI), the Natural Sciences and Engineering Research Council (NSERC), the National Research Council (NRC), the Canadian Institutes of Health Research (CIHR), the Government of Saskatchewan, and the University of Saskatchewan. Discussions with John McElhone resulting in the selection of 19th century daguerreotypes from NGC and private collection is gratefully acknowledged. Research conducted at Western University is supported by CFI, NSERC, and CRC (Canada Research Chair).

References

[1] Marcy. Dinius, Daguerreotype," encyclopedia of nineteenth-century photography, in: John Hannavy, New York: Routledge, 2008, pp. 367–372.
[2] McElhone John, in: Processes and Formats," The Extended Moment: Fifty Years of Collecting Photographs at the National Gallery of Canada, Ann Thomas and John McElhone. Ottawa: Canadian Photography Institute of the National Gallery of Canada, 2018, p. 250.
[3] Naomi. Rosenblum, in: A World History of Photography, Abbeville Press, New York, 1997, pp. 39–52. third edition.
[4] Camfield Willis, Willis Deirdre, History of Photography: Techniques and Equipment, London: Toronto; Hamlyn, 1980.
[5] I. Foster, The daguerreotype, PhotoLife 44 (2019) 46.
[6] C.M. Prieto, Protecting daguerreotypes: a new structural housing system (SHS), J. Inst. Conserv. 40 (2017) 226.
[7] E. Grieten, O. Schalm, P. Tack, S. Bauters, P. Storme, N. Gauquelin, J. Caen, A. Patelli, L. Vincze, D. Schryvers, Reclaiming the image of daguerreotypes: characterization of the corroded surface before and after atmospheric plasma treatment, J. Cult. Herit. 28 (2017) 56–64.
[8] A. Fischer, G. Eggert, R. Dinnebier, T. Runcevski, When glass and metal corrode together, V: sodium copper formate, Study. *Conserv.* 63 (2018) 342.
[9] E.A. Marquis, Y.M. Chen, J. Kohanek, Y. Dong, S.A. Centeno, Exposing the sub–surface of historical daguerreotypes and the effects of sulfur-induced corrosion, Corros. Sci. 94 (2015) 438.
[10] W. Wei, I. Gerritsen, C. Waldthausen, Re-examining the (electro-)chemical cleaning of daguerreotypes: Microscopic Chang Vs. Macroscopic Perception, Top. Photogr. Preserv. 14 (2011) 24.
[11] M.S. Barger, D.K. Barger, W.B. White, Characterization of corrosion products on old protective glass, especially daguerreotype cover glasses, J. Mater. Sci. 24 (1989) 1343.
[12] M.S. Barger, W.B. White, The Daguerreotype: Nineteenth-Century Technology and Modern Science, The Smithsonian Institute, Washington, DC, USA, 1991.
[13] M.S. Kozachuk, T.K. Sham, R.R. Martin, A.J. Nelson, I. Coulthard, J.P. McElhone, Recovery of degraded-beyond recognition 19th century daguerreotypes with rapid high dynamic range elemental X-ray fluorescence imaging of mercury L emission, Sci. Rep. 8 (2018) 1.
[14] M.S. Kozachuk, Synchrotron Radiation Analysis of Daguerreotypes: Surface Characterization, Electrocleaning, and Preservation Ph.D. Thesis, The University of Western Ontario, London, ON, Canada, 2019.
[15] Smieska M.S. Kozachuk, T.K. Sham, R.R. Martin, A.J. Nelson, I. Coulthard, A.R Woll, Recovering past reflections: X-ray fluorescence imaging of electro-cleaned 19th century daguerreotypes, Heritage 2 (2019) 568.
[16] M.S. Kozachuk, T.K. Sham, R.R. Martin, A.J. Nelson, I. Coulthard, Exploring tarnished daguerreotypes with synchrotron light: XRF and μ-XANES analysis, Herit. Sci. 6 (2018) 12.
[17] M.S. Kozachuk, M.O. Aviles, R.R. Martin, B. Potts, T.K. Sham, F. Lagugne-Labarthet, Imaging the surface of a hand-colored 19th century daguerreotype, Appl. Spectrosc. 72 (2018) 1215.
[18] A. Stark, F. Filice, J.J. Noël, R.R. Martin, T.K. Sham, Y.Z. Finfrock, S.M Heald, Retrieving tarnished daguerreotype content using X-ray fluorescence imaging-recent observations on the effect of chemical and electrochemical cleaning methods, Herit. *Sci.* 4 (2021) 1605–1615.
[19] M. Cotte, J. Susini, V.A. Sole´, Y. Taniguchi, J. Chillida, E. Emilie Checroune, P. Walter, Applications of synchrotron-based micro-imaging techniques to the chemical analysis of ancient paintings, J. Anal. At. Spectrom. 23 (2008) 820–828.
[20] M. Cotte, A. Genty-Vincent, J. Koen, J Susini, Applications of synchrotron X-ray nano-probes in the field of cultural heritage, C.R. Physique 19 (2018) 575–588.
[21] K, J. Dik, Koen Janssens, G. van der Snickt, L. van der Loeff, K.;. Rickers, M Cotte, Visualization of a lost painting by vincent van gogh using synchrotron radiation based X-ray fluorescence elemental mapping, Anal. Chem. 8 (0) (2006) 6436–6442.
[22] U. Bergmann, P.L. Manning, R.A. Wogelius, Chemical mapping of paleontological and archeological artifacts with synchrotron X-rays, Ann. Rev. Anal. Chem. 5 (2012) 361–389.
[23] P.L. Manning, N.P. Edwards, R.A. Wogelius, U. Bergmann, H.E. Barden, P.L. Larson, D. Schwarz-Wings, V.M. Egerton, D. Sokaras, R.A. Mori, W.I. Sellerse, Synchrotron-based chemical imaging reveals plumage patterns in a 150 million year old early bird, J. Anal. At. Spectrom. 28 (2013) 1024.
[24] P.L. Manning, N.P. Edwards, U. Bergmann, J. Anné, W.I. Sellers, A. van Veelen, D. Sokaras, V.M. Egerton, R. Alonso-Mori, K. Ignatyev, B.E. van Dongen, K. Wakamatsu, S. Ito, F. Knoll, R.A. Wogelius, Pheomelanis pigment remnants mapped in fossils of an extinct mammal, Nat. Comm. 10 (2019) 2250.
[25] L. Bertrand, S. Bernard, F. Marone, M. Thoury, I. Reiche, A. Gourrier, P. Sciau, U. Bergmann, Emerging approaches in synchrotron studies of materials from cultural and natural history collections, Top Curr. Chem. (Z) (2016), doi:10.1007/s41061-015-0003-1.
[26] D. Creagh, D. Bradley editors, Physical Techniques in the Study of Art, Archaeology and Cultural Heritage, 2, Elsevier, Amsterdam, The Netherlands, 2007.
[27] Janet Buerger, in: French Daguerreotypes, Chicago: University of Chicago Press, 1989, pp. 50–66.
[28] D.L. S.M. Heald, J.O. Crossa, D.L. Brewe, R.A. Gordon R.A.;, The PNC/XOR X-ray microprobe station at APS sector 20, Nucl. Instrum. Methods Phys. Res. A 582 (2007) 215–217.
[29] Q. Xiao, A. Maclennan, Y. Hu, Y.M. Hackett, Leinweber, T.K. Sham, Medium-energy microprobe station at the SXRMB of the CLS, *J. Synchrotron Rad.* 24 (2017) 333–337.
[30] A. Reinhardt, R. Feng, Q. Xiao, Y.F. Hu, T.K. Sham, Exploring the Dzi bead with synchrotron light: XRD, XRF imaging and [micro]-XANES analysis, Herit. Sci 2 (2020) 1035–1045.
[31] R. A.R. Woll, J. Mass, C. Bisulca, R. Huang, D.H. Bilderback, S. Gruner, N. Gao, Development of confocal X-ray fluorescence (XRF) microscopy at the Cornell high energy synchrotron source, Appl. Phys. A 83 (2006) 235–238.
[32] S. Heald, G.T. Seidler, D. Mortensen, B. Mattern, A. Joseph, J.A. Bradley, N. Hess, M.;. Bowden, Recent tests of X-ray spectrometers using polycapillary optics, in: Proc. SPIE 8502, *Advances in X-Ray/EUV Optics and Components VII*, 2012, p. 85020I.
[33] Heather Wagner, Synchrotron radiation and cultural heritage, Synchrotron Radiat. News 35 (5) (2022) 2.
[34] C. Dudley, D. Bradley, Physical Techniques in the Study of Art, Archaeology and Cultural Heritage, 2, Elsevier, 2007.